Med Chem Res
DOI 10.1007/s00044-016-1672-1

MEDICINAL CHEMISTRY RESEARCH

ORIGINAL RESEARCH

Design and synthesis of new 2,5-disubstituted-1,3,4-oxadiazole analogues as anticancer agents

Mohit Agarwal[1] · Vikram Singh[1] · Sachin Kumar Sharma[1] · Piush Sharma[1] · Md. Yousuf Ansari[2] · Surender Singh Jadav[3] · Sabina Yasmin[3] · Reddymasu Sreenivasulu[4] · Mohd. Zaheen Hassan[5] · Vipin Saini[6] · Mohamed Jawed Ahsan[1]

Received: 19 December 2015 / Accepted: 4 July 2016

Abstract In continuance of our search for new anticancer agents, we report herein the design, synthesis, and anticancer evaluation of oxadiazole analogues. Two series (**4a-h** and **4i-q**) of new oxadiazole analogues were designed based on heterocyclic (1,3,4-oxadiazole)-linked aryl core of IMC-038525 (tubulin polymerization inhibitor), NSC 776715, and NSC 776715 and synthesized. All the compounds were fully characterized by infrared, nuclear magnetic resonance spectroscopy, and mass spectral data and the purity of compounds was checked by elemental analysis (C, H, and N analysis). Further seven compounds were evaluated for anticancer activity on nine different panels of 60 cell lines (60 NCI cancer cell lines) according to the National Cancer Institute screening protocol and percent growth and percent growth inhibition was calculated at 10 μM drug concentration. Ten compounds were evaluated for anticancer activity on two cancer cell lines (HeLa and MDA-MB-435) as per the standard protocol reported at four different drug concentrations (10^{-7}, 10^{-6}, 10^{-5}, and 10^{-4} μM) and GI_{50}, LC_{50}, and TGI dose-related parameters were calculated. The compound **4j** showed maximum anticancer activity at 10 μM, and was found to have higher sensitivity against MOLT-4, IGROV1, HCT-116, and K-562 with percent growth inhibitions of 50.38, 48.45, 46.26, and 46.26 respectively. The compound **4j** showed superior anticancer activity than imatinib on 41 human cancer cell lines. The compound **4p** showed anticancer activity with GI_{50} of 36.7 and 46.5 μM against HeLa and MDA-MB-435 cell lines, respectively.

Keywords Anticancer · Adriamycin · IMC-038525 · Oxadiazole · One dose assay · Cancer cell lines

Introduction

Cancer is a disease associated with uncontrolled cell growth and proliferation and is responsible for nearly 13 % of total death tolls worldwide. A total of 1,658,370 new cancer cases and 589,430 cancer deaths are projected to occur in the United States in 2015 (Siegel et al., 2015). In India the total number of cancer cases are likely to go up from 979,786 cases in the year 2010 to 1,148,757 cases in the year 2020 (Takiar et al., 2010). In spite of considerable advancement in the understanding of molecular mechanisms of cancer pathogenesis, yet no specific treatment is available to alleviate the disease completely. Despite the availability of improved drugs and targeted cancer therapies, it is expected that the new cases of cancer will jump to

Mohit Agarwal and Vikram Singh contributed to this work equally.

✉ Mohamed Jawed Ahsan
jawedpharma@gmail.com

[1] Department of Pharmaceutical Chemistry, Maharishi Arvind College of Pharmacy Ambabri Circle, Jaipur, Rajasthan 302 039, India

[2] Pharmacoinformatics Department, National Institute of Pharmaceutical Education and Research (NIPER), Hajipur 844 102 Bihar, India

[3] Department of Pharmaceutical Chemistry, Birla Institute of Technology, Mesra, Ranchi, Jharkhand 835 215, India

[4] Department of Chemistry, , Acharya Nagarjuna University, Nagarjuna Nagar 522 510 Andhra Pradesh, India

[5] School of Chemical Science, University Sains Malaysia, Penang 118 00, Malaysia

[6] M. M. College of Pharmacy, Maharishi Markandeshwar University, Mullana, Ambala, Haryana 133207, India

Published online: 01 August 2016

19.3 million worldwide by 2025 (WHO World Cancer Report, 2014). The therapeutic approach of cancer includes chemotherapy, radiotherapy, surgery, immunotherapy, monoclonal antibody therapy, hormonal therapy, targeted therapy, and angiogenesis inhibition. In chemotherapy the chemo-preventive molecules act by various molecular mechanisms and may involve inhibition of initiation, promotion, progression, and metastasis of cancerous cells, but this process can also kill the normal cells. The use of anticancer drugs not only affects the normal human cells but are also restricted to their toxic potentials, resistance, and genotoxicity. Due to these complications the demand for relatively more effective and safer agents for cancer therapy is today's need to combat against cancer (Aydemir and Bilaloglu, 2003).

The heterocyclic oxadiazoles being rich in biological potential as antitubercular (Karabanovich et al., 2016), anticancer (Abdel-Aziz et al., 2016), anticonvulsant (Rajak et al., 2013), antimicrobial (Bakht et al., 2010), anti-HIV (Khan et al., 2012), anti-inflammatory (Ramaprasad et al., 2013) inspired us to go further and explore oxadiazoles . Moreover, 1,3,4-oxadiazole heterocycles are very good bioisosteres of amides and esters, and to a large extent enhance the pharmacological activity by participating in hydrogen bonding interactions with receptors (Zhang et al., 2014). In the present investigation the heterocyclic (oxadiazole) linked aryl core of IMC-038525 (tubulin polymerization inhibitor), NSC 776715, and NSC 776716 was taken and two newer series of oxadiazoles (**4a-g** and **4i-o**) were synthesized (Tuma et al., 2010; Ahsan et al., 2014). The design of the title compounds (**4a-g** and **4i-o**) is shown in Fig. 1. Furthermore, the aryl group of the title compounds (**4a-g**) was replaced with five-member heteroaryl (2-furyl) group (**4h**) in the first series of oxadiazoles. The second series of oxadiazoles (**4i-q**) was designed with the incorporation of methylene linker with a hope to increase the pharmacological profile. The methylene linker (-CH_2-) is suggested to offer flexibility to the molecule due to sp^3 hybridization and would result in increased pharmacological activity. The terminal aryl group (**4i-o**) was further replaced with five-member heteroaryl (2-furyl) group (**4p**) and aliphatic alkyl (ethyl) group (**4q**) (Fig.2).

Experimental

General

All the chemicals were procured from Merck (Mumbai) and S.D. Fine Chemicals (Mumbai). Melting points were determined by open tube capillary method and are uncorrected. Purity of the compounds was checked on thin layer chromatography (TLC) plates (silica gel G) using mobile phase chloroform/methanol (8:2) and toluene/ethylacetate/formic acid (5:4:1); the spots were located under iodine vapor or UV light. Infra spectra were obtained on a Schimadzu 8201 PC, FT-IR spectrometer (KBr pellets). ^{1}H NMR and ^{13}C NMR spectra were recorded on a Bruker AC 400 MHz spectrometer using Tetramethylsilane as internal standard in dimethylsulphoxide (DMSO)d_6. Mass spectra were recorded on a Bruker Esquire LCMS using ESI and elemental analyses were performed on Perkin-Elmer 2400 Elemental Analyzer.

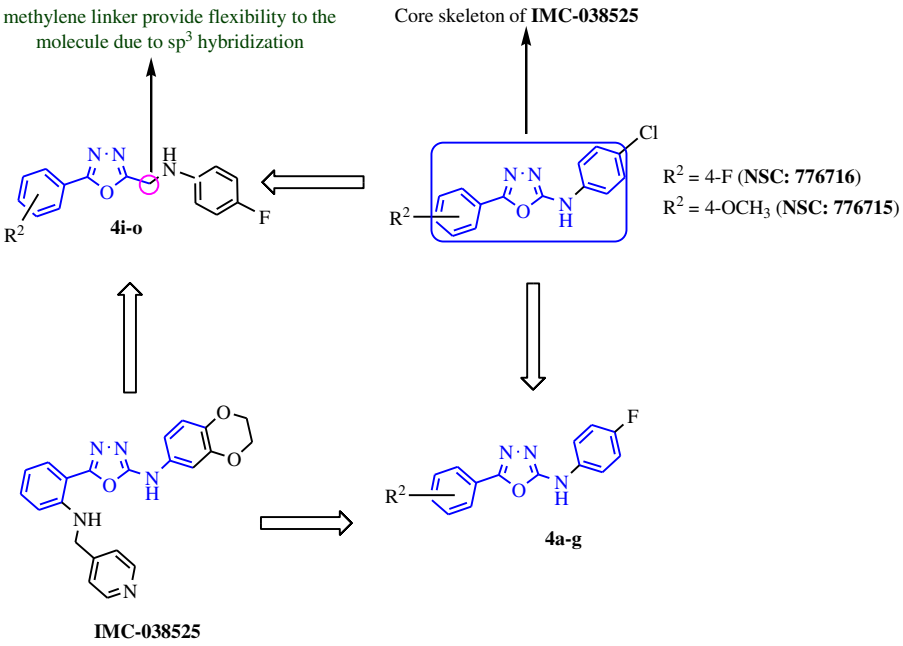

Fig. 1 Rationally design template for target molecules obtained from anticancer drugs IMC-038525, and reported compounds (Ahsan et al., 2014)

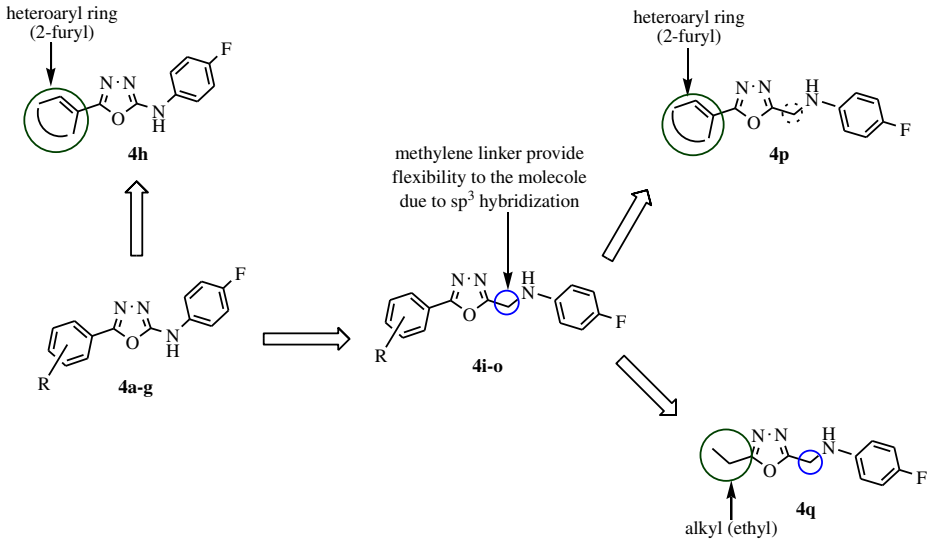

Fig. 2 Rationale template and modification for target molecules and introduction of methylene linkage (-CH_2-) to provide flexibility

Method for the synthesis of 4-fluorophenyl urea (2a)

4-Fluoro aniline (**1**) (0.1 mol; 11.1 g) was dissolved in 20 ml glacial acetic acid and 10 ml hot water, and sodium cyanate (0.1 mol; 6.5 g) in 80 ml of hot water was added with stirring. It was then allowed to stand for 30 min, then cooled in ice bath, filtered with suction, dried, and recrystallized from boiling water to obtain 4-fluorophenyl urea (**2a**) (Azam et al., 2010).

Method for the synthesis of 4-fluorophenyl semicarbazide (3a)

Equimolar quantities of 4-fluorophenyl urea (**2a**) (0.05 mol; 7.70 g) and hydrazine hydrate (AR 99–100 %) (0.05 mol; 2.5 ml) in 50 ml ethanol were refluxed for 24 h with stirring. The two-thirds volume of alcohol was distilled by vacuum distillation and then the reaction mixture was poured into the crushed ice. The resultant precipitate was filtered, washed with water, and dried. The solid mass was recrystallized from 25 ml absolute ethanol to obtain 4-fluorophenyl semicarbazide (**3**) (Azam et al., 2010).

General method for the synthesis of N-(4-fluorophenyl)-5-aryl-1,3,4-oxadiazol-2-amine analogues (4a-h)

4-Fluorophenyl semicarbazide (0.005 mol; 0.85 g) (**3a**) and aromatic aldehydes (0.005 mol) were refluxed for 10–12 h using 20 mol% $NaHSO_3$ and ethanol-water system (1:2, v/v) solvent (Sangshetti et al., 2011). After completion of reaction, the excess solvent was removed and the concentrate was poured into crushed ice filter, washed with water, dried, and recrystallized with absolute ethanol to obtain the final product (**4a–x**). The reaction was monitored throughout by TLC using chloroform/ methanol (8:2) and acetone/n-hexane (8:2) as mobile phase.

*N,5-Bis(4-fluorophenyl)-1,3,4-oxadiazol-2-amine (**4a**)*

IR (KBr) ν_{max}: 3352 (NH), 1511 (C=N), 1252 (C–O–C, oxadiazole stretch), 786 (C–F) cm^{-1}; ^{1}H NMR (400 MHz, DMSO-d_6): δ 7.21–7.24 (2H, d, $J = 8.8$ Hz, ArH), 7.27–7.29 (2H, d, $J = 8.8$ Hz, ArH), 7.47–7.49 (2H, d, $J = 4.9$ Hz, ArH), 7.62–7.63 (2H, d, $J = 4.9$ Hz, ArH), 8.81 (1H, s, ArNH); ^{13}C NMR (100 MHz, DMSO-d_6): δ 162.2, 164.9, 152.1, 149.3, 138.9, 129.6, 121.2, 117.4, 116.8, 116.2; EIMS $m/z = 274$ $[M]^+$, 276 $[M+2]^+$. Cal/Ana: [C (61.54) 61.58 H (3.32) 3.23 N (15.38) 15.32].

*5-(4-Chlorophenyl)-N-(4-fluorophenyl)-1,3,4-oxadiazol-2-amine (**4b**)*

IR (KBr) ν_{max}: 3334 (NH), 1507 (C=N), 1249 (C–O–C, oxadiazole stretch), 806 (C–F), 694 (C–Cl) cm^{-1}; ^{1}H NMR (400 MHz, DMSO-d_6): δ 7.11–7.13 (2H, d, $J = 8.8$ Hz, ArH), 7.45–7.47 (2H, d, $J = 8.3$ Hz, ArH), 7.61–7.62 (2H, d, $J = 4.9$ Hz, ArH), 7.85–7.88 (2H, d, $J = 8.4$ Hz, ArH), 8.98 (1H, s, ArNH); ^{13}C NMR (100 MHz, DMSO-d_6): δ 164.2, 152.9, 149.3, 138.9, 134.7, 129.9, 128.7, 124.4, 117.8, 116.1; EIMS $m/z = 290$ $[M]^+$, 292 $[M+2]^+$, 294 $[M+4]^+$. Cal/Ana: [C (58.02) 58.06 H (3.13) 3.16 N (14.51) 14.42].

*4-{5-[(4-Fluorophenyl)amino]-1,3,4-oxadiazol-2-yl}phenol (**4c**)*

IR (KBr) ν_{max}: 3412 (OH), 3334 (NH), 1508 (C=N), 1243 (C–O–C, oxadiazole stretch), 794 (C–F) cm^{-1}; ^{1}H NMR (400 MHz, DMSO-d_6): δ 7.02–7.04 (2H, d, $J = 8.1$ Hz, ArH), 7.35–7.37 (2H, d, $J = 8.1$ Hz, ArH), 7.60–7.62 (2H,

d, $J = 8.2$ Hz, ArH), 7.85–7.87 (2H, d, $J = 8.2$ Hz, ArH), 8.91 (1H, s, ArNH), 10.52 (1H, s, OH); ^{13}C NMR (100 MHz, DMSO-d_6): δ 164.3, 158.7, 152.4, 149.3, 138.6, 128.9, 118.4, 117.8, 116.9, 116.1; EIMS $m/z = 272$ $[M]^+$, 274 $[M+2]^+$. Cal/Ana: [C (61.99) 62.00 H (3.72) 3.75 N (15.49) 15.52].

*2-{5-[(4-Fluorophenyl)amino]-1,3,4-oxadiazol-2-yl}phenol (**4d**)*

IR (KBr) ν_{max}: 3424 (OH), 3324 (NH), 1507 (C=N), 1263 (C–O–C, oxadiazole stretch), 796 (C–F) cm^{-1}; ^{1}H NMR (400 MHz, DMSO–d_6): δ 7.05–7.07 (2H, d, $J = 8.0$ Hz, ArH), 7.23–7.25 (2H, d, $J = 8.0$ Hz, ArH), 7.63–7.82 (4H, m, ArH), 8.87 (1H, s, ArNH), 10.49 (1H, s, OH); ^{13}C NMR (100 MHz, DMSO-d_6): δ 164.3, 155.2, 152.4, 149.1, 138.2, 130.1, 128.1, 121.8, 117.9, 116.9, 116.3, 112.5; EIMS $m/z = 272$ $[M]^+$, 274 $[M+2]^+$. Cal/Ana: [C (61.99) 67.00 H (3.72) 3.75 N (15.49) 15.52].

*N-(4-Fluorophenyl)-5-(4-methoxyphenyl)-1,3,4-oxadiazol-2-amine (**4e**)*

IR (KBr) ν_{max}: 3380 (NH), 1510 (C=N), 1253 (C–O–C, oxadiazole stretch), 1168 (O–CH_3), 806 (C–F) cm^{-1}; ^{1}H NMR (400 MHz, DMSO-d_6): δ 3.77 (3H, s, OCH_3), 6.94–6.96 (2H, d, $J = 8.2$ Hz, ArH), 7.02–7.04 (2H, d, $J = 8.2$ Hz, ArH), 7.62–7.64 (2H, d, $J = 8.0$ Hz, ArH), 7.75–7.77 (2H, d, $J = 8.0$ Hz, ArH), 8.67 (1H, s, ArNH); ^{13}C NMR (100 MHz, DMSO-d_6): δ 164.0, 160.1, 152.0, 149.9, 138.7, 128.5, 118.5, 117.9, 116.3, 114.9, 56.2; EIMS $m/z = 285$ $[M]^+$, 286 $[M+1]^+$. Cal/Ana: [C (63.15) 63.19 H (4.24) 4.25 N (14.73) 14.76].

*5-(3,4-Dimethoxyphenyl)-N-(4-fluorophenyl)-1,3,4-oxadiazol-2-amine (**4f**)*

IR (KBr) ν_{max}: 3368 (NH), 1512 (C=N), 1250 (C–O–C, oxadiazole stretch), 1167 (O–CH_3), 806 (C–F) cm^{-1}; ^{1}H NMR (400 MHz, DMSO-d_6): δ 3.80 (6H, s, OCH_3), 7.04–7.06 (2H, d, $J = 8.1$ Hz, ArH), 7.11–7.13 (2H, d, $J = 8.2$ Hz, ArH), 7.62–7.66 (2H, m, ArH), 7.85 (1H, s, ArH), 8.61 (1H, s, ArNH); ^{13}C NMR (100 MHz, DMSO-d_6): δ 164.5, 152.1, 150.2, 149.9, 149.1, 138.7, 120.5, 119.5, 117.1, 116.6, 115.8, 112.7, 56.2; EIMS $m/z = 315$ $[M]^+$, 316 $[M+1]^+$. Cal/Ana: [C (60.95) 60.91 H (4.48) 4.45 N (13.33) 13.36].

*4-{5-[(4-Fluorophenyl)amino]-1,3,4-oxadiazol-2-yl}-2-methoxyphenol (**4g**)*

IR (KBr) ν_{max}: 3412 (OH), 3328 (NH), 1507 (C=N), 1252 (C–O–C, oxadiazole stretch), 1167 (O–CH_3), 802 (C–F) cm^{-1}; ^{1}H NMR (400 MHz, DMSO-d_6): δ 3.77 (3H, s, OCH_3), 6.94–6.96 (2H, d, $J = 8.0$ Hz, ArH), 7.02–7.04 (2H, d, $J = 8.0$ Hz, ArH), 7.38 (1H, s, ArH), 7.61–7.64 (2H, m, ArH), 8.72 (1H, s, ArNH), 10.56 (1H, s, OCH_3); ^{13}C NMR (100 MHz, DMSO-d_6): δ 164.3, 152.1, 151.2, 149.9, 145.1, 138.1, 121.2, 119.9, 117.9, 117.3, 116.3, 112.3, 56.6; EIMS $m/z = 301$ $[M]^+$, 302 $[M+1]^+$. Cal/Ana: [C (59.80) 59.90 H (4.01) 3.98 N (13.95) 13.96].

*N-(4-Fluorophenyl)-5-(furan-2-yl)-1,3,4-oxadiazol-2-amine (**4h**)*

IR (KBr) ν_{max}: 3333 (NH), 1509 (C=N), 1254 (C–O–C, oxadiazole stretch), 802 (C–F) cm^{-1}; ^{1}H NMR (400 MHz, DMSO-d_6): δ 6.92–6.94 (2H, d, $J = 8.1$ Hz, ArH), 6.97–6.99 (2H, d, $J = 8.1$ Hz, ArH), 7.06–7.12 (3H, m, ArH), 8.48 (1H, s, ArNH); ^{13}C NMR (100 MHz, DMSO-d_6): δ 157.3, 152.1, 149.9, 147.4, 142.9, 117.9, 116.3, 105.3, 107.7; EIMS $m/z = 245$ $[M]^+$, 246 $[M+1]^+$. Cal/Ana: [C (58.78) 58.80 H (3.29) 3.27 N (17.14) 17.16].

Method for the synthesis of ethyl [(4-fluorophenyl) amino]acetate (2b)

4-Fluoroaniline (**1**) (0.1 mol; 11.1 g) and ethylchoroacetate (0.2 mol; ~24 ml) were taken in a round bottom flask and suspended in 100 ml ethanol and (0.15 mol; ~20.1 g) anhydrous sodium acetate trihydrate was added to the mixture. The mixture was refluxed for 48 h on sand bath with vigorous stirring, then cooled and the excess solvent removed under reduced pressure. The residual mass was triturated with ice water to remove sodium acetate trihydrate and extracted with ethylacetate (3 × 50 ml) and the ethylacetate layer was washed with 10 % sodium hydroxide solution (3 × 30 ml) followed by water (3 × 30 ml) and then dried over anhydrous sodium sulphate and evaporated to dryness to obtain ethyl[(4-fluorophenyl)amino]acetate (**2b**) as light brown solid (Finger et al., 1965).

Method for the synthesis of 2-[(4-fluorophenyl)amino] acetohydrazide (3b)

Ethyl[(4-fluorophenyl)amino]acetate (**2b**) (0.075 mol; 14.79 g) and hydrazine hydrate (0.15 mol; ~7.5 ml) was refluxed in ethanol for 22 h on water bath. The two-third volume of reaction mixture was removed under reduced pressure and then poured into crushed ice to obtain 2-[(4-chlorophenyl)amino]acetohydrazide (**4**) as light brown solid (Finger et al., 1965).

General method for the synthesis of N-(4-fluorophenyl) [5-aryl/alkyl-1,3,4-oxadiazol-2-yl]methyl amine analogues (4i-q)

2-[(4-Fluorophenyl)amino]acetohydrazide (**3b**) (0.001 mol; 0.91 g) and aromatic/aliphatic aldehydes was refluxed in ethanol-water system (1:2, v/v) solvent and 20 mol% $NaHSO_3$ for 10–12 h (Sangshetti et al., 2011). After completion of reaction the excess solvent was removed and the concentrate was poured into crushed ice filter, washed with water, dried and recrystallized with absolute ethanol to obtain the final product (**4i-q**). The completion of reaction was monitored throughout by TLC using chloroform/methanol (8:1) and acetone/n-hexane (8:2) as mobile phase.

*4-Fluoro-N-{[5-(4-fluorophenyl)-1,3,4-oxadiazol-2-yl] methyl}aniline (**4i**)*

IR (KBr) ν_{max}: 3349 (NH), 1509 (C=N), 1256 (C–O–C, oxadiazole stretch), 802 (C–F) cm^{-1}; ^1H NMR (400 MHz, DMSO-d_6): δ 4.32 (2H, s, CH_2), 6.92–6.94 (2H, d, $J = 8.1$ Hz, ArH), 6.98–7.00 (2H, d, $J = 8.1$ Hz, ArH), 7.07–7.08 (2H, d, $J = 4.9$ Hz, ArH), 7.85–7.86 (2H, d, $J = 4.9$ Hz, ArH), 8.53 (1H, s, ArNH); ^{13}C NMR (100 MHz, DMSO-d_6): δ 164.2, 162.9, 151.1, 149.3, 143.9, 129.6, 121.2, 116.8, 116.2, 115.9, 51.6; EIMS $m/z = 287$ $[M]^+$, 288 $[M+1]^+$. Cal/Ana: [C (62.72) 62.78 H (3.86) 3.85 N (14.63) 14.59].

*N-{[5-(4-Chlorophenyl)-1,3,4-oxadiazol-2-yl]methyl}-4-fluoroaniline (**4j**)*

IR (KBr) ν_{max}: 3343 (NH), 1512 (C=N), 1251 (C–O–C, oxadiazole stretch), 806 (C–F), 696 (C–Cl) cm^{-1}; ^1H NMR (400 MHz, DMSO-d_6): δ 4.35 (2H, s, CH_2), 6.91–6.93 (2H, d, $J = 8.0$ Hz, ArH), 6.99–7.01 (2H, d, $J = 8.0$ Hz, ArH), 7.37–7.38 (2H, d, $J = 4.9$ Hz, ArH), 7.65–7.66 (2H, d, $J = 4.9$ Hz, ArH), 8.69 (1H, s, ArNH); ^{13}C NMR (100 MHz, DMSO-d_6): δ 164.3, 151.1, 149.7, 143.8, 129.6, 128.2, 124.4, 116.8, 115.9, 51.6; EIMS $m/z = 303$ $[M]^+$, 305 $[M+2]^+$. Cal/Ana: [C (59.32) 59.28 H (3.65) 3.66 N (13.84) 13.89].

*4-(5-{[(4-Fluorophenyl)amino]methyl}-1,3,4-oxadiazol-2-yl)phenol (**4k**)*

IR (KBr) ν_{max}: 3421 (OH), 3312 (NH), 1509 (C=N), 1253 (C–O–C, oxadiazole stretch), 802 (C–F) cm^{-1}; ^1H NMR (400 MHz, DMSO-d_6): δ 4.35 (2H, s, CH_2), 6.71–6.73 (2H, d, $J = 8.0$ Hz, ArH), 6.82–6.84 (2H, d, $J = 8.1$ Hz, ArH), 6.94–7.38 (4H, m, ArH), 8.61 (1H, s, ArNH), 10.51 (1H, s, OH); ^{13}C NMR (100 MHz, DMSO-d_6): δ 165.4, 155.5, 151.9, 149.5, 143.8, 130.6, 128.5, 121.9, 116.9, 116.3, 115.1, 51.4; EIMS $m/z = 285$ $[M]^+$, 286 $[M+1]^+$. Cal/Ana: [C (63.15) 63.10 H (4.24) 4.26 N (14.73) 14.76].

*2-(5-{[(4-Fluorophenyl)amino]methyl}-1,3,4-oxadiazol-2-yl)phenol (**4l**)*

IR (KBr) ν_{max}: 3429 (OH), 3349 (NH), 1507 (C=N), 1252 (C–O–C, oxadiazole stretch), 804 (C–F) cm^{-1}; ^1H NMR (400 MHz, DMSO-d_6): δ 4.32 (2H, s, CH_2), 6.81–6.83 (2H, d, $J = 8.3$ Hz, ArH), 6.93–6.95 (2H, d, $J = 8.3$ Hz, ArH), 7.08–7.10 (2H, d, $J = 8.1$ Hz, ArH), 7.67–7.69 (2H, d, $J = 8.1$ Hz, ArH), 8.52 (1H, s, ArNH), 10.42 (1H, s, OH); ^{13}C NMR (100 MHz, DMSO-d_6): δ 164.5, 158.5, 151.3, 149.7, 143.2, 128.8, 118.2, 116.8, 116.1, 115.3, 51.6; EIMS $m/z = 285$ $[M]^+$, 286 $[M+1]^+$. Cal/Ana: [C (63.15) 63.12 H (4.24) 4.26 N (14.73) 14.72].

*4-Fluoro-N-{[5-(4-methoxyphenyl)-1,3,4-oxadiazol-2-yl] methyl}aniline (**4m**)*

IR (KBr) ν_{max}: 3270 (NH), 1508 (C=N), 1249 (C–O–C, oxadiazole stretch), 1166 (O–CH_3), 813 (C–F) cm^{-1}; ^1H NMR (400 MHz, DMSO-d_6): δ 3.80 (3H, s, OCH_3), 4.30 (2H, s, CH_2), 7.02–7.04 (2H, d, $J = 8.1$ Hz, ArH), 7.23–7.25 (2H, d, $J = 8.1$ Hz, ArH), 7.63–7.65 (2H, d, $J = 8.0$ Hz, ArH), 7.85–7.87 (2H, d, $J = 8.0$ Hz, ArH), 8.61 (1H, s, ArNH); ^{13}C NMR (100 MHz, DMSO-d_6): δ 164.3, 160.9, 151.9, 149.3, 138.7, 128.7, 118.4, 117.7, 116.4, 114.2, 56.2, 51.6; EIMS $m/z = 299$ $[M]^+$, 300 $[M+1]^+$. Cal/Ana: [C (64.21) 64.19 H (4.71) 4.72 N (14.04) 14.06].

*N-{[5-(3,4-Dimethoxyphenyl)-1,3,4-oxadiazol-2-yl]methyl}-4-fluoroaniline (**4n**)*

3318 (NH), 1512 (C=N), 1253 (C–O–C, oxadiazole stretch), 1167 (O–CH_3), 804 (C–F) cm^{-1}; ^1H NMR (400 MHz, DMSO-d_6): δ 3.81 (3H, s, OCH_3), 3.85 (3H, s, OCH_3), 4.31 (2H, s, CH_2), 7.11–7.13 (2H, d, $J = 8.1$ Hz, ArH), 7.22–7.24 (2H, d, $J = 8.1$ Hz, ArH), 7.66 (1H, s, ArH), 7.72–7.74 (2H, d, $J = 8.3$ Hz, ArH), 8.61 (1H, s, ArNH); ^{13}C NMR (100 MHz, DMSO-d_6): δ 164.3, 160.6, 152.1, 149.8, 138.6, 128.5, 118.6, 117.9, 116.3, 114.9, 56.2, 51.6; EIMS $m/z = 329$ $[M]^+$, 330 $[M+1]^+$. Cal/Ana: [C (62.00) 62.05 H (4.90) 4.88 N (12.76) 12.74].

*4-(5-{[(4-Fluorophenyl)amino]methyl}-1,3,4-oxadiazol-2-yl)-2-methoxyphenol (**4o**)*

IR (KBr) ν_{max}: 3412 (OH), 3328 (NH), 1507 (C=N), 1252 (C–O–C, oxadiazole stretch), 1167 (O–CH_3), 802 (C–F) cm^{-1}; ^1H NMR (400 MHz, DMSO-d_6): δ 3.81 (3H, s, OCH_3), 4.32 (2H, s, CH_2), 6.91–6.93 (2H, d, $J = 8.1$ Hz, ArH), 7.05–7.06 (2H, d, $J = 8.1$ Hz, ArH), 7.41 (1H, s,

ArH), 7.61–7.63 (2H, d, $J = 8.2$ Hz, ArH), 8.67 (1H, s, ArNH), 10.52 (1H, s, OH); ^{13}C NMR (100 MHz, DMSO-d_6): δ 164.3, 152.5, 151.9, 149.2, 145.8, 138.7, 121.1, 119.9, 117.3, 117.1, 116.4, 112.2, 56.6, 52.6; EIMS $m/z =$ 315 $[M]^+$, 316 $[M+1]^+$. Cal/Ana: [C (60.95) 60.91 H (4.48) 4.50 N (13.33) 13.36].

*4-Fluoro-N-{[5-(furan-2-yl)-1,3,4-oxadiazol-2-yl]methyl} aniline (**4p**)*

IR (KBr) ν_{max}: 3331 (NH), 1507 (C=N), 1249 (C–O–C, oxadiazole stretch), 804 (C–F) cm^{-1}; ^{1}H NMR (400 MHz, DMSO-d_6): δ 4.32 (2H, s, CH_2), 6.91–6.93 (2H, d, $J = 8.2$ Hz, ArH), 6.98–7.00 (2H, d, $J = 8.2$ Hz, ArH), 7.09–7.18 (3H, m, ArH), 8.68 (1H, s, ArNH); ^{13}C NMR (100 MHz, DMSO-d_6): δ 157.6, 152.3, 149.5, 147.3, 142.7, 117.7, 116.4, 105.8, 107.7, 52.6; EIMS $m/z = 259$ $[M]^+$, 260 $[M+1]^+$. Cal/Ana: [C (60.23) 60.28 H (3.89) 3.87 N (16.21) 16.19].

*N-[(5-Ethyl-1,3,4-oxadiazol-2-yl)methyl]-4-fluoroaniline (**4q**)*

IR (KBr) ν_{max}: 3321 (NH), 1507 (C=N), 1250 (C–O–C, oxadiazole stretch), 806 (C–F) cm^{-1}; ^{1}H NMR (400 MHz, DMSO-d_6): δ 1.34–1.39 (3H, m, CH_3), 2.55–2.59 (2H, m, CH_2), 4.31 (2H, s, CH_2), 6.93–6.95 (2H, d, $J = 8.1$ Hz, ArH), 6.97–6.99 (2H, d, $J = 8.1$ Hz, ArH), 8.61 (1H, s, ArNH); ^{13}C NMR (100 MHz, DMSO-d_6): δ 156.6, 152.3, 149.5, 143.3, 116.4, 115.8, 52.6, 23.1, 14.9; EIMS $m/z =$ 221 $[M]^+$, 222 $[M+1]^+$. Cal/Ana: [C (59.72) 59.76 H (5.47) 5.50 N (18.99) 18.93].

In vitro anticancer activity

The anticancer screening was carried out on nine different panels of cancer cell lines viz. leukemia, melanoma, lung, colon, CNS, ovarian, renal, prostate, and breast cancers cell lines, nearly 60 in number according to the reported NCI US protocol (http://dtp.nci.nih.gov; Boyd and Paull, 1995; Monks et al., 1991; Shoemaker 2006). Seven compounds (**4b**, **4e**, **4f**, **4i**, **4j**, **4m**, and **4n**) were selected for anticancer screening at National Cancer Institute (NCI), USA. NCI selected the compounds for anticancer screening based on the novelty of heterocyclic ring system, drug-like properties utilizing the concept of privileged scaffolds, structure based on computer-aided drug design, etc., while the structures containing problematic linkage or functional groups (e.g. nitro, nitroso, -N-N-, -N=N-, imine, semicarbazone, thiamides, thioureas) are avoided (http://dtp.nci.nih.gov). Using the seven absorbance measurements (time zero (T_i), control growth (C), and test growth in the presence of drug at the five concentration levels (T_f)), the percentage growth was calculated at each of the drug concentrations levels as: $[(T_f - T_i)/(C - T_i)] \times 100$ for concentrations for which $T_f \geq T_i$ and $[(T_f - T_i)/T_i] \times 100$ for concentrations for which $T_f < T_i$.

Anticancer activity of the 10 compounds (**4a**, **4c**, **4d**, **4g**, **4h**, **4k**, **4l**, **4o**, **4p**, and **4q**) was estimated in two different human cell lines (HeLa and MDA-MB-435) using the sulforhodamine B (SRB) protocol (Vichai and Kirtikara, 2006; Prabhakaran et al., 2014). The cells were inoculated into 96-well microtiter plates (90 µl/well) at appropriate plating densities depending on the doubling time of individual cell lines. The microtiter plates were incubated at 37 °C in a carbon dioxide (CO_2) incubator for 24 h prior to addition of experimental drugs. The cells were then incubated for 48 h with the test compounds and the experiment was concluded by adding 30 % chilled trichloro acetic acid to the wells. Cells were stained using 0.4 % SRB in 1 % acetic acid. The SRB dye bound to the fixed cells was eluted using 10 mM unbuffered Tris solution and the optical density was measured using enzyme-linked immunosorbent assay micro plate reader. Percent growth (GP) was calculated on a plate-by-plate basis for test wells relative to control wells and was expressed as the ratio of average absorbance of the test well to the average absorbance of the control wells multiplied by 100. Using the six absorbance measurements (time zero (T_z), control growth (C), and test growth in the presence of drug at the four concentration levels (T_i)], the percentage growth was calculated at each of the drug concentration levels. Percentage growth inhibition was calculated using the formulae

$$\left[\frac{Ti - Tz}{C - Tz}\right] \times 100 \text{ for concentrations } Ti \geq Tz \text{ i.e.}$$

$$Ti - Tz \text{ is positive or zero}$$

$$\left[\frac{Ti - Tz}{Tz}\right] \times 100 \text{ for concentrations } Ti < Tz \text{ i.e.}$$

$$Ti - Tz \text{ is negative}$$

Three-dose response parameters (GI_{50}, TGI, and LC_{50}) were calculated for each of the experimental agents. Growth inhibition of 50 % (GI_{50}) was calculated from $100 \times [(T_i - T_z)/(C - T_z)] = 50$, which was the drug concentration resulting in a 50 % reduction in the net protein increase (as measured by sulforhodamine B, SRB staining) in control cells during the drug incubation. The total growth inhibition (TGI) was calculated from $T_i = T_z$, which was the drug concentration resulting in TGI and signified the cytostatic effect. The LC_{50} was calculated from $100 \times [(T_i - T_z)/(C - T_z)] = -50$, which was the drug concentration resulting in a net loss of cells following treatment which indicated the concentration of drug resulting in a 50 % reduction in the measured protein at the end of the drug treatment as compared to that at the beginning.

Results and discussion

Chemistry

The title compounds (**4a-q**) were synthesized as per the synthetic protocol outlined in Schemes 1 and 2 and thier physical constants are given in Table 1. The oxadiazole analogues of the series (**4a-h**) was synthesized starting from 4-fluroaniline (**1**). In the initial step 4-fluorophenyl urea (**2a**) was synthesized from 4-fluroaniline (**1**) and sodium cyanate in the glacial acetic acid as per the reported method (Azam et al., 2010). In the subsequent step 4-fluorophenyl urea (**2a**) and hydrazine hydrate was refluxed in ethanol for 24 h to obtain 4-fluorophenyl semicarbazide (**3a**). In the final step equimolar quantity of 4-fluorophenyl semicarbazide (**3a**) and aromatic aldehydes was refluxed for 10–12 h using 20 mol% $NaHSO_3$ and ethanol-water system (1:2, v/v) solvent to obtain *N*-(4-fluorophenyl)-5-aryl-1,3,4-oxadiazol-2-amine analogues (**4a-h**). The oxadiazoles of the series (**4i-q**) were synthesized starting from 4-fluoroaniline. In the initial step equimolar quantity of 4-fluoroaniline (**1**) (0.1 mol; 11.1) and ethylchoroacetate (0.2 mol; ~24 ml) were taken in a round bottom flask and suspended in 80–100 ml ethanol and anhydrous sodium acetate trihydrate (0.15 mol; ~20.1 g) was added to the mixture. The mixture was refluxed for 48 h on sand bath with vigorous stirring to obtain intermediate semisolid ethyl[(4-fluorophenyl)amino] acetate (**2b**). In the subsequent step compound **3b** (0.075 mol; 14.79 g) and hydrazine hydrate (0.15 mol; ~7.5 ml) was refluxed in ethanol for 22 h on water bath to obtain 2-[(4-fluorophenyl)amino]acetohydrazide (**3b**) as light brown solid (Finger et al., 1965). In the final step equimolar quantity of 2-[(4-fluorophenyl)amino]acetohydrazide (**3a**) and aromatic/aliphatic aldehyde was refluxed for 10–12 h in ethanol-water system (1:2, v/v) solvent using 20 mol% $NaHSO_3$ to obtain *N*-(4-fluorophenyl)[5-aryl/alkyl-1,3,4-oxadiazol-2-yl]methyl amine analogues (**4i-q**). The completion of reaction was monitored throughout by TLC using mobile phase chloroform/methanol (8:2), acetone/n-hexane (8:2), and toluene/ethylacetate/formic acid (5:4:1) and the spots were identified either in iodine vapor or UV chamber. The yields of the title compounds were ranging between 62 and 85 % after recrystallization with absolute ethanol. The oxadiazole analogues (**4a-q**) were synthesized as per the reported method (Sangshetti et al., 2011).

The structures of the newly synthesized compounds were confirmed by using modern analytical techniques viz. FT-IR, NMR (^{1}H and ^{13}C), and mass spectral data. The purity of the synthesized compounds was checked by elemental analysis (C, H, and N analysis). Both the analytical and spectral data of the compounds were in full agreement with the proposed structure. In general, the IR spectra of the compounds afforded oxadiazole stretching (C-O-C) at 1243–1263 cm^{-1}, C=N stretching at 1507–1512 cm^{-1} and NH stretching at 3270–3349 cm^{-1} while OH stretching was observed at 3412–3429 cm^{-1} bands. In the Nuclear Magnetic Resonance spectra (^{1}H NMR) the signals of the respective protons of the oxadiazole analogues (**4a-q**) were verified on the basis of their chemical shifts, multiplicities, and coupling constants in DMSO-d_6. The spectra of the

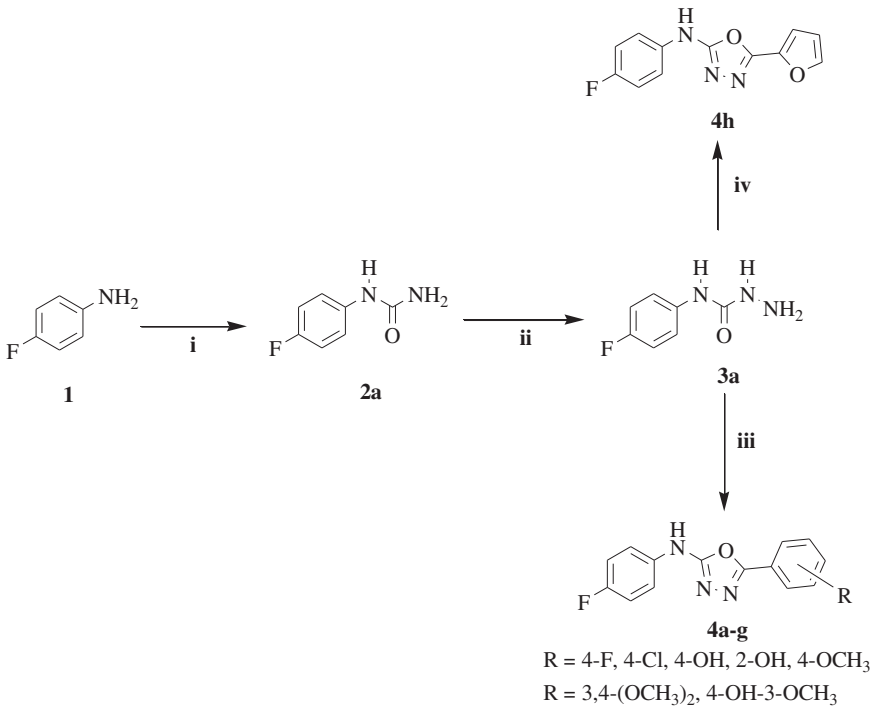

Scheme 1 Protocol for the synthesis of *N*-(4-fluorophenyl)-5-aryl-1,3,4-oxadiazol-2-amine analogues (**4a-h**): (i) Reagents: NaCNO/AcOH; (ii) $NH_2NH_2H_2O$/EtOH; (iii) and (iv) ArCHO/ 20 mol% $NaHSO_3$/ EtOH-H_2O system (1:2, v/v)

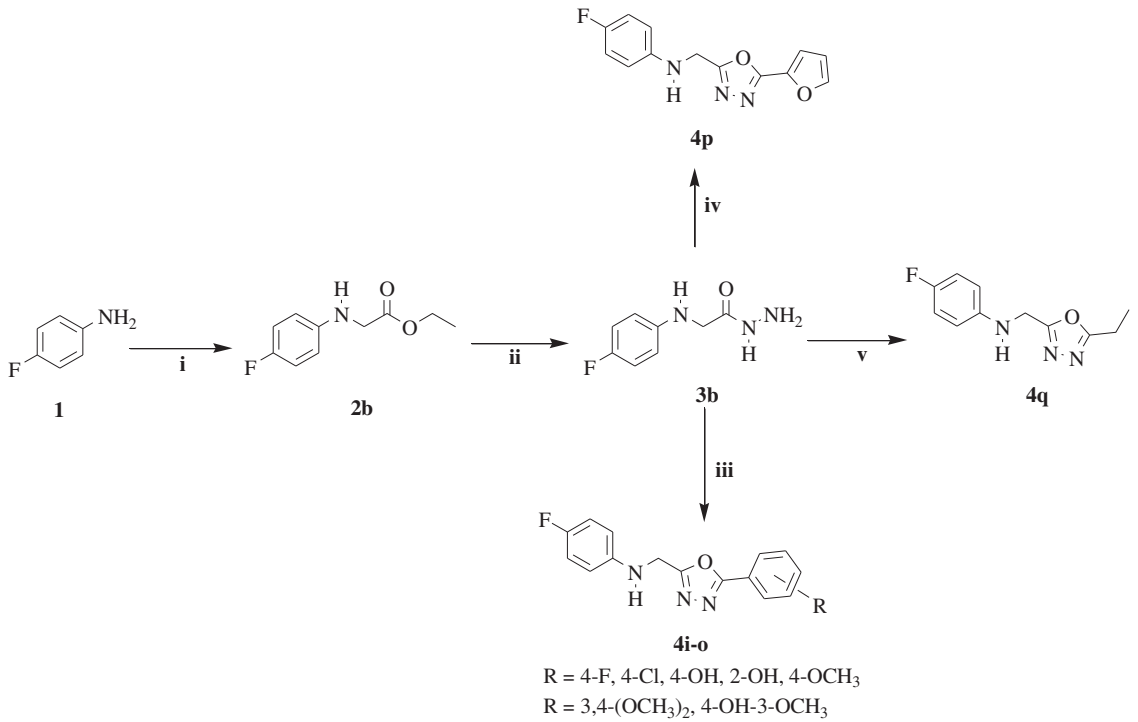

Scheme 2 Protocol for the synthesis of *N*-(4-fluorophenyl)[5-aryl/alkyl-1,3,4-oxadiazol-2-yl]methyl amine analogues (**4i-q**): (i) Reagents: $ClCH_2COOEt$; sodium acetate trihydrate/ EtOH; (ii) $NH_2NH_2H_2O$/EtOH; (iii), (iv) and (v) ArCHO/RCHO/ 20 mol% $NaHSO_3$/EtOH-H_2O system (1:2, v/v)

compounds showed a singlet at δ 3.77–3.85 ppm corresponding to OCH_3 group; a singlet at δ 4.30–4.35 ppm corresponding to methylene (-CH_2-) linkage; singlet/doublet/multiplet at δ 6.92–7.88 ppm corresponding to aromatic protons (ArH); a singlet at 8.52–8.98 ppm corresponding to aromatic NH (ArNH) and a singlet at 10.42–10.56 ppm corresponding to phenolic (OH) group. The nature of carbon atoms was characterized and verified by ^{13}C NMR, while the mass spectra of the compounds showed molecular ion peak M+, $(M+1)^+$,and $(M+2)^+$.

Anticancer activity

Seven compounds (**4b**, **4e**, **4f**, **4i**, **4j**, **4m,** and **4n**) were evaluated for their anticancer activity as per the NCI US standard protocol at single dose assay (10 μM concentration) on leukemia, melanoma, lung, colon, CNS, ovarian, renal, prostate, and breast cancers cell lines (nearly 60 in numbers) and growth percent (GP) and percent growth inhibition (%GI) were calculated. Ten compounds (**4a**, **4c**, **4d**, **4g**, **4h**, **4i**, **4k**, **4l**, **4o,** and **4p**) were evaluated for anticancer activity on HeLa (Cervix) and MDA-MB-435 (Breast) cancer cell lines at four different drug concentration (10^{-7}, 10^{-6}, 10^{-5}, and 10^{-4} μM) and three-dose response parameters (GI_{50}, TGI, and LC_{50}) were calculated. The compound **4b** showed maximum sensitivity towards CCRF-CEM and T-47D with %GIs of 41.55 and 37.80, respectively. The compound **4e** showed maximum sensitivity towards T-47D, K-562, A498, NCI-H522, PC-3, and HCT-116 with percent GIs of 44.70, 43.63, 40.94, 39.54, 38.84, and 32.58, respectively. The compound **4i** showed maximum sensitivity towards MDA-MB-231/ATCC, NCI-H522, and A549/ATCC with percent GIs of 41.48, 41.39, and 33.28, respectively. The compound **4m** showed maximum sensitivity towards T-47D, UO-31, and HCT-116 with percent GIs of 43.68, 38.24, and 32.77, respectively. The compound **4n** showed maximum sensitivity towards T-47D, PC-3, UO-31, K562, RPMI-8226, and HOP-92 with percent GIs of 46.11, 44.06, 39.88, 38.55, 33.86, and 32.96, respectively. The compounds **4b**, **4e**, **4f**, **4i**, and **4n** showed moderate activity; however, the compound **4m** showed mean growth percent (GP) of 90.29 but found to be inactive towards cancer cell lines. The compound **4j** showed maximum sensitivity towards MOLT-4, IGROV1, HCT-116, K-562, RPMI-8226, PC-3, UO-31, MCF-7, MDA-MB-231/ATCC, NCI-H522, MDA-MB-468, T-47D, A549/ATCC, and HOP-92 with percent GIs of 50.38, 48.45, 46.26, 46.25, 45.94, 45.73, 45.67, 44.86, 44.43, 43.50, 43.12, 43.01, 33.87, and 32.95, respectively. The compound **4j** showed comparatively higher activity among the series (**4a-q**) (Table 2). The compound that showed growth inhibitions of ≥32 % was considered to be active towards that particular cell lines and marked with bold figure in Table 2 (Corona et al., 2009). When

Table 1 The physical constants of the of 2,5–disubstituted–1,3,4–oxadiazole analogues (**4a–q**)

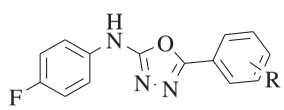

4a-g

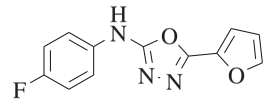

4h

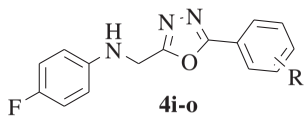

4i-o

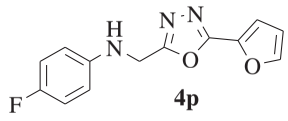

4p

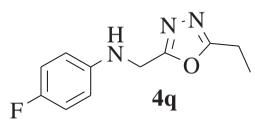

4q

S. No.	Compound	R	NSC Code	R_f	% Yield	Mp (°C)
1	**4a**	4–Fluoro–	–	0.59[a]	74	178–180
2	**4b**	4–Chloro–	784594	0.70[a]	70	170–172
3	**4c**	4–Hydroxy–	–	0.65[a]	75	158–160
4	**4d**	2–Hydroxy–	–	0.65[a]	79	148–150
5	**4e**	4–Methoxy–	784595	0.68[a]	72	130–132
6	**4f**	3,4–Dimethoxy–	784596	0.78[a]	80	162–164
7	**4g**	4–Hydroxy–3–methoxy–	–	0.67[a]	78	188–190
8	**4h**	–	–	0.62[a]	62	142–144
9	**4i**	4–Fluoro–	785214	0.85[b]	65	100–102
10	**4j**	4–Chloro–	784597	0.70[b]	77	70–72
11	**4k**	4–Hydroxy–	–	0.60[b]	65	98–100
12	**4l**	2–Hydroxy–	–	0.84[b]	70	78–80
13	**4m**	4–Methoxy–	784598	0.78[b]	75	88–90
14	**4n**	3,4–Dimethoxy–	784599	0.64[b]	76	96–98
15	**4o**	4–Hydroxy–3–methoxy–	–	0.71[b]	85	104–106
16	**4p**	—	–	0.81[b]	75	92–94
17	**4q**	–	–	0.79[b]	78	110–112

[a] Chloroform/methanol (8:2)

[b] Toluene/ethylacetate/formic acid (5:4:1)

Table 2 In vitro anticancer activity of 2,5-disubstituted-1,3,4-oxadiazole analogues (**4a-q**)

Compound	Cancer cell lines assay in single dose assay 10 μM concentration				
	Mean growth percent (GP)	Range of GP	The most sensitive cell lines	GP of the most sensitive cell line	% growth inhibition (GI)
4a	117.6	116.9-118.3	HeLa (Cervix Cancer)	118.3	−18.3
			MDA-MB-435 (Breast Cancer)	116.9	−16.9
4b	95.15	58.45-137.03	CCRF-CEM (Leukemia)	**58.45**	**41.55**
			T-47D (Breast Cancer)	**66.20**	**37.80**
			K-562 (Leukemia)	70.64	29.36
			NCI-H522 (Non-Small Cell Lung Cancer)	74.03	25.97
			MCF-7 (Breast Cancer)	75.43	24.57
			SK-OV-3 (Renal Cancer)	77.42	22.58
4c	109.2	97.7-120.7	HeLa (Cervix Cancer)	97.7	2.3
			MDA-MB-435 (Breast Cancer)	120.7	−20.7
4d	110.1	105.4-114.8	HeLa (Cervix Cancer)	105.4	−5.4
			MDA-MB-435 (Breast Cancer)	114.8	−14.8
4e	85.81	55.30-131.98	T-47D (Breast Cancer)	**55.30**	**44.70**
			K-562 (Leukemia)	**56.37**	**43.63**
			A498 (Renal Cancer)	**59.06**	**40.94**
			NCI-H522 (Non-Small Cell Lung Cancer)	**60.42**	**39.58**
			PC-3 (Prostate cancer)	**61.16**	**38.84**
			HCT-116 (Colon Cancer)	**67.42**	**32.58**
			HT29 (Colon Cancer)	68.60	31.40
			A549/ATCC (Non-Small Cell Lung Cancer)	69.74	30.26
4f	99.13	80.63-114.27	HOP-92 (Non-Small Cell Lung Cancer)	80.63	19.37
			PC-3 (Prostate cancer)	82.37	17.63
			NCI-H226 (Non-Small Cell Lung Cancer)	85.19	14.81
			RPMI-8226 (Leukemia)	87.39	12.61
			SNB-75 (CNS cancer)	87.70	12.30
4g	122.6	117.8-127.4	HeLa (Cervix Cancer)	127.4	−27.4
			MDA-MB-435 (Breast Cancer)	117.8	−17.8
4h	119.8	116-123.7	HeLa (Cervix Cancer)	116.0	−16.0
			MDA-MB-435 (Breast Cancer)	123.7	−23.7
4i	89.47	58.52-118.31	MDA-MB-231/ATCC (Breast Cancer)	**58.52**	**41.48**
			NCI-H522 (Non-Small Cell Lung Cancer)	**58.61**	**41.39**
			A549/ATCC (Non-Small Cell Lung Cancer)	**66.72**	**33.28**
			U251 (CNS cancer)	68.64	31.36
			HS 578T (Breast Cancer)	70.34	29.66
			UACC-257 (Melanoma)	70.86	29.14
4j	76.12	49.62-126.50	MOLT-4 (Leukemia)	**49.62**	**50.38**
			IGROV1 (Ovarian Cancer)	**51.55**	**48.45**
			HCT-116 (Colon Cancer)	**53.74**	**46.26**
			K-562 (Leukemia)	**53.75**	**46.25**
			RPMI-8226 (Leukemia)	**54.06**	**45.94**
			PC-3 (Prostate cancer)	**54.27**	**45.73**
			UO-31 (Renal Cancer)	**54.33**	**45.67**
			MCF-7 (Breast Cancer)	**55.16**	**44.86**
			MDA-MB-231/ATCC (Breast Cancer)	**55.57**	**44.43**
			NCI-H522 (Non-Small Cell Lung Cancer)	**56.50**	**43.50**
			MDA-MB-468 (Breast Cancer)	**56.88**	**43.12**
			T-47D (Breast Cancer)	**56.99**	**43.01**
			A549/ATCC (Non-Small Cell Lung Cancer)	**66.13**	**33.87**
			HOP-92 (Non-Small Cell Lung Cancer)	**67.05**	**32.95**

Table 2 continued

Compound	Cancer cell lines assay in single dose assay 10 μM concentration				
	Mean growth percent (GP)	Range of GP	The most sensitive cell lines	GP of the most sensitive cell line	% growth inhibition (GI)
4k	119.1	110.2-127.9	HeLa (Cervix Cancer)	110.2	110.2
			MDA-MB-435 (Breast Cancer)	127.9	−27.9
4l	116.7	114-119.4	HeLa (Cervix Cancer)	119.4	−19.4
			MDA-MB-435 (Breast Cancer)	114.0	−14.0
4m	90.29	56.32-118.03	T-47D (Breast Cancer)	**56.32**	**43.68**
			UO-31 (Renal Cancer)	**61.76**	**38.24**
			HCT-116 (Colon Cancer)	**67.23**	**32.77**
			SK-OV-3 (Ovarian Cancer)	70.58	29.42
			HOP-62 (Non-Small Cell Lung Cancer)	71.23	28.77
4n	87.65	53.89-137.74	T-47D (Breast Cancer)	**53.89**	**46.11**
			PC-3 (Prostate cancer)	**55.94**	**44.06**
			UO-31 (Renal Cancer)	**60.12**	**39.88**
			K-562 (Leukemia)	**61.65**	**38.35**
			RPMI-8226 (Leukemia)	**66.14**	**33.86**
			HOP-92 (Non-Small Cell Lung Cancer)	**67.04**	**32.96**
			IGROV1 (Ovarian Cancer)	68.79	31.21
			MDA-MB-231/ATCC (Breast Cancer)	69.80	30.20
4o	113.1	106.7-119.5	HeLa (Cervix Cancer)	106.7	−6.7
			MDA-MB-435 (Breast Cancer)	119.5	−19.5
4p	120.6	119.3-122	HeLa (Cervix Cancer)	119.3	119.3
			MDA-MB-435 (Breast Cancer)	122.0	−22.0
4q	118.3	114.1-122.5	HeLa (Cervix Cancer)	114.1	−14.1
			MDA-MB-435 (Breast Cancer)	122.5	−22.5

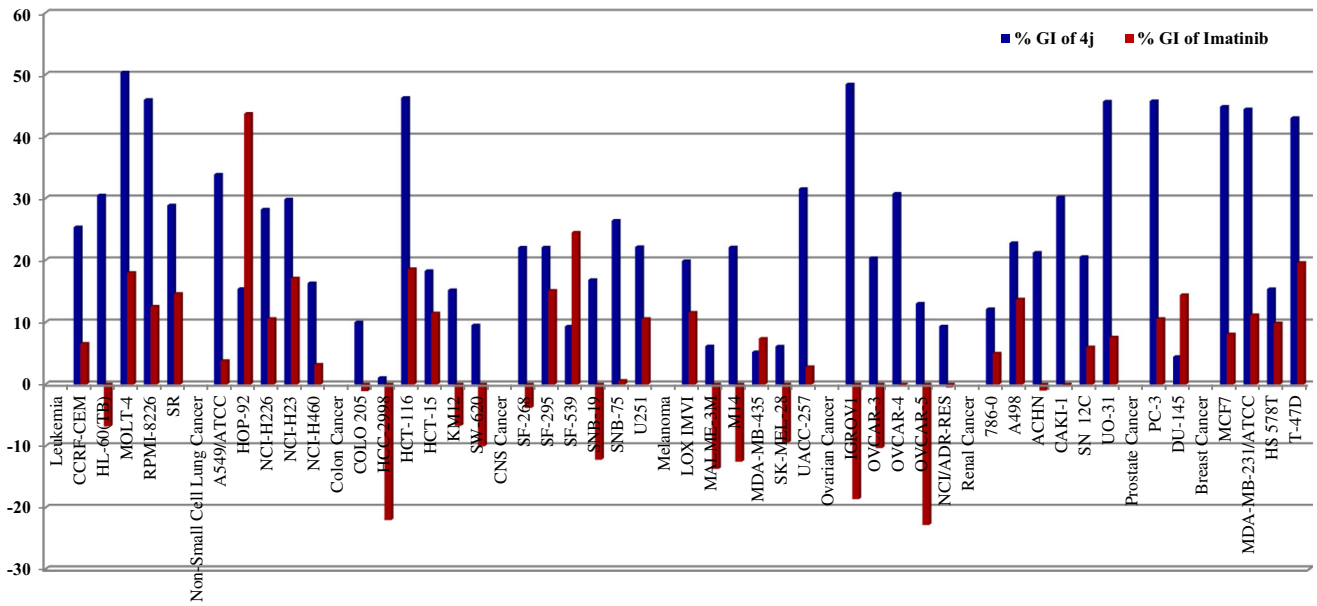

Fig. 3 The comparison of percent growth inhibition (% GI) expressed by compound **4j** and Imatinib against the NCI human cancer cell lines at 10 μM

compared with the standard drug imatinib, the compound **4j** showed superior anticancer activity over nearly 41 cancer cell lines. The comparison of %GIs expressed by compound **4j** (blue) and imatinib (red) is shown in Fig. 3. The compounds **4a**, **4c**, **4d**, **4g**, **4h**, **4k**, **4l** **4o**, **4p**, and **4q** showed less anticancer activity with mean growth percent

Table 3 The percent control growth of selected compounds at different molar concentrations

Compound	% control growth							
	Molar drug concentrations							
	HeLa				MDA-MB-435			
	10^{-7} M	10^{-6} M	10^{-5} M	10^{-4} M	10^{-7} M	10^{-6} M	10^{-5} M	10^{-4} M
4a	107.6	118.3	116.9	62.2	118.9	116.9	110.9	86.1
4c	109.7	97.7	107.1	−13.1	116.8	120.7	108.8	33.9
4d	94.1	105.4	112.3	83.5	117.0	114.8	114.7	87.2
4g	113.7	127.4	120.5	−29.6	118.0	117.8	113.7	59.9
4h	110.2	116.0	115.1	64.7	122.5	123.7	118.1	86.7
4k	105.1	110.2	104.7	30.2	127.7	127.9	126.0	85.6
4l	121.2	119.4	89.3	**−40.3**	114.3	114.0	112.6	74.9
4o	104.5	106.7	94.1	21.0	123.9	119.5	113.2	83.9
4p	107.2	119.3	45.0	−26.3	120.9	122.0	100.4	−30.1
4q	95.7	114.1	110.1	37.7	121.2	122.5	120.4	83.8
ADR	−74.8	−72.7	−71.0	**−29.4**	10.7	49.8	−70.7	**−65.3**

ADR Adriamycin

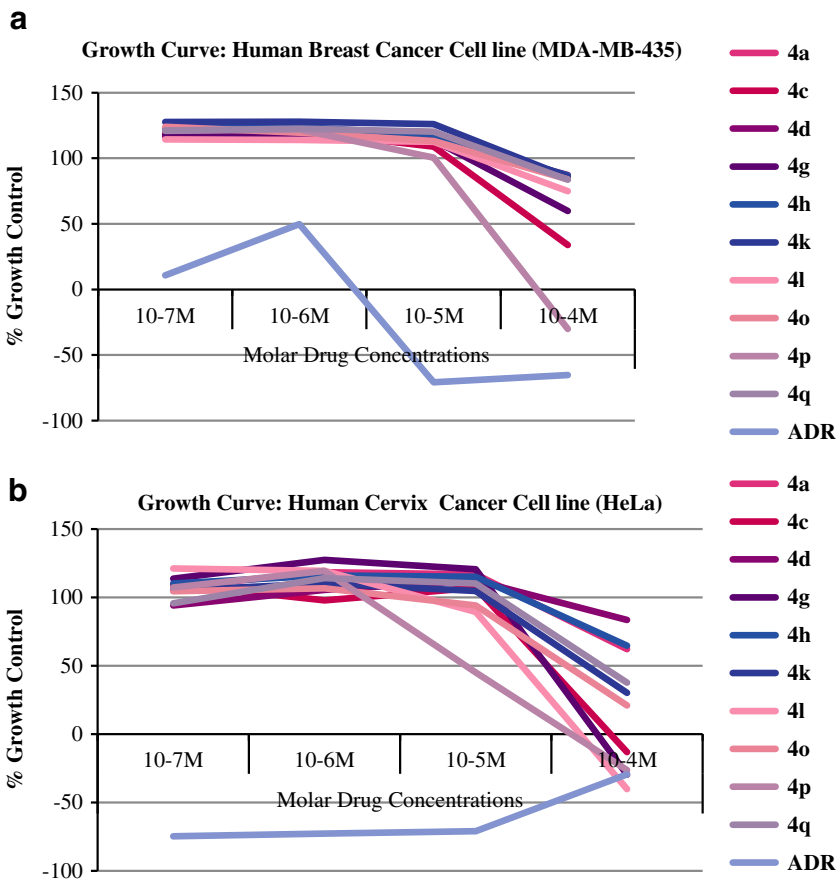

Fig. 4 **a** Growth curve of selected oxadiazole analogues over MDA-MB-435 (Human Breast Cancer cell line) at different molar concentrations (μM). **b** Growth curve of selected oxadiazole analogues over HeLa (Human Cervix Cancer cell line) at different molar concentrations (μM)

of 109.1–20.6 at 10 μM and the anticancer activity of compounds was found to be increased with increase in concentration (100 μM). The compound **4l** showed higher anticancer activity than standard drug adriamycin at 100 μM against HeLa cell lines while compound **4p** showed maximum sensitivity against MDA-MB-435 cell lines at 100 μM but comparatively less active than standard drug adriamycin. The anticancer activity of 10 compounds

a

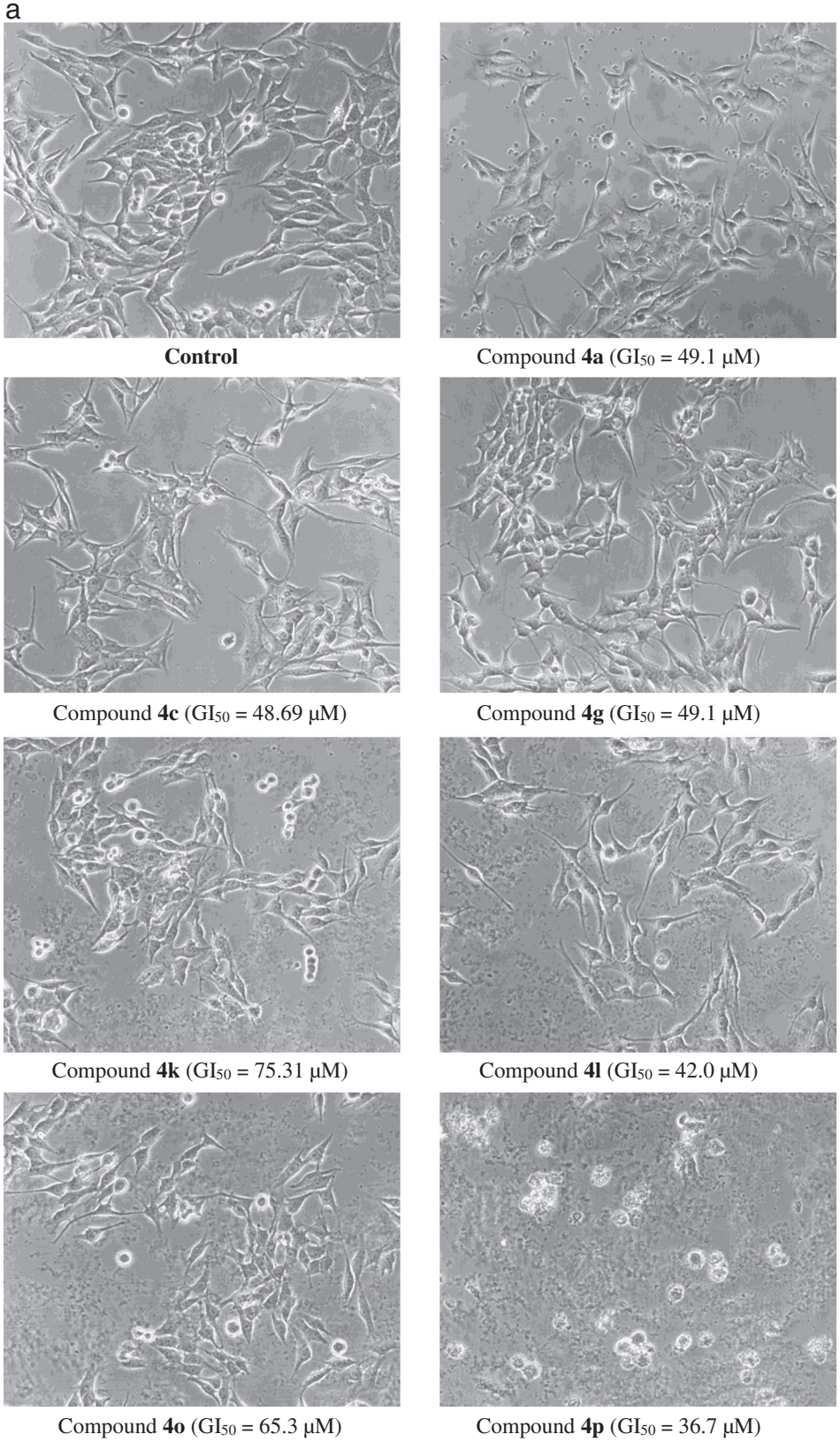

Fig. 5 **a** Images of growth control of MDA-MB-435 cancer cell line by oxadiazole analogues. **b** Images of growth control of HeLa cancer cell line by oxadiazole analogues

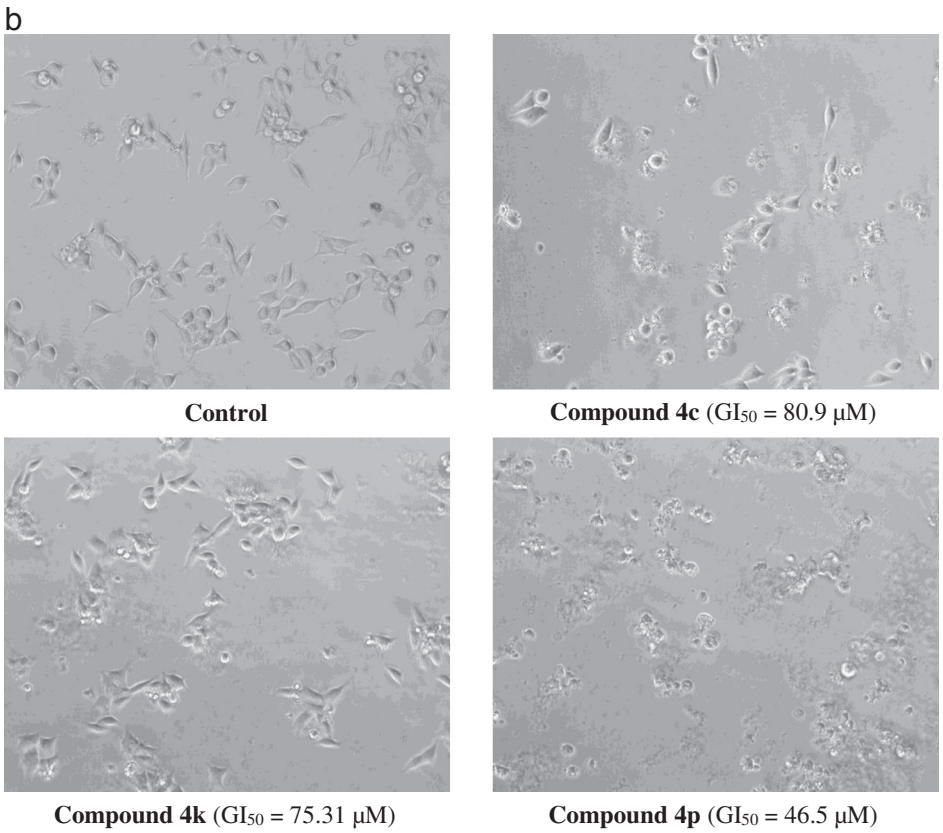

Fig. 5 Continued

Table 4 Calculated values of LC_{50}, TGI, and GI_{50} of the selected oxadiazole analogues

Compound	Micro molar drug concentrations calculated from graph					
	HeLa			MDA-MB-435		
	LC_{50}	TGI	GI_{50}	LC_{50}	TGI	GI_{50}
4a	>100	81.5	49.1	>100	>100	>100
4c	>100	89.95	48.69	>100	>100	80.9
4d	>100	>100	>100	>100	>100	>100
4g	>100	81.5	49.1	>100	>100	>100
4h	>100	>100	>100	>100	>100	>100
4k	>100	>100	75.31	>100	>100	75.31
4l	>100	73.75	42	>100	>100	>100
4o	>100	>100	65.3	>100	>100	>100
4p	>100	76.3	36.7	>100	76.3	46.5
4q	>100	>100	83.8	>100	>100	>100
ADR	54.42	<0.1	<0.1	70.6	1.7	<0.1

ADR Adriamycin

against HeLa and MDA-MB-435 at four different concentrations (10^{-7}, 10^{-6}, 10^{-5}, and 10^{-4} μM) is given in Table 3. The graphical presentation of growth curve of 10 oxadiazole analogues at different molar concentrations (μM) is shown in Fig. 4a (MDA-MB-435) and Fig. 4b (HeLa).

Ten compounds (**4a**, **4c**, **4d**, **4g**, **4h**, **4i**, **4k**, **4l**, **4o,** and **4p**) were evaluated for anticancer activity on HeLa (Cervix) and MDA-MB-435 (Breast) cancer cell lines at four different drug concentration (10^{-7}, 10^{-6}, 10^{-5}, and 10^{-4} μM) and three-dose response parameters (GI_{50}, TGI, and LC_{50}) were calculated (Table 4). The compound **4p** showed anticancer activity having GI_{50} of 36.7 μM against HeLa and 46.5 μM against MDA-MB-435 cell lines. The LC_{50} was found to be > 100 μM for both the cell lines; however, TGI value were ranging between 81.5 and > 100 μM over HeLa and 76.3 and > 100 μM over MDA-MB-435 cell lines. The images of growth control over cancer cell lines by 10 oxadiazoles are shown in Fig. 5a (MDA-MB-435) and Fig 5b (HeLa).

The structure activity relationship was established with the anticancer data. The oxadiazole-linked aryl nucleus with 4-chloro substitution showed maximum anticancer activity and followed by 4-fluoro, 4-methoxy and 3,4-dimethoxy substitution. Substitution with 4-hydroxy and 2-hydroxy was not very significant. The order of pharmacological activity followed as 4-Cl > 4-F > 4-OCH_3 > 3,4-$(OCH_3)_2$. The replacement of aryl ring with either five heteroaryl (2-furyl) or alkyl group reduced the anticancer activity. Furthermore, introduction of the methylene (-CH_2-) linkage was found to increase the

anticancer activity. The reason for increased anticancer activity might be due to flexibility offered to the molecule due to sp^3 hybridization.

Conclusion

Two series of oxadiazoles were synthesized with and without methylene linkage (-CH_2-) in satisfactory yield. All the oxadiazole analogues were evaluated for their anticancer screening as per the NCI US standard protocol. Some of the oxadiazoles showed significant anticancer activity in one dose assay at 10 μM. Furthermore, introduction of methylene (-CH_2-) was found to be promising in improving biological profile. Among the series of oxadiazoles, the compound **4j** showed anticancer activity superior to that of the standard drug Imatinib over 41 cancer cell lines could be considered as lead for further optimization and drug discovery.

Acknowledgments Antiproliferative data were provided by National Cancer Institute (NCI US), Bethesda, MD, USA and Anticancer Drug Screening Facility (ACTREC), Navi Mumbai, India. We are grateful for all help provided by Prof. Doug Smallwood and Mr. Mohammed Nayel NCI US), Bethesda, MD, USA. We are also grateful for all help provided by Dr. Jyoti Kode, ACTREC, Navi Mumbai, India. The people holding the management of Maharishi Arvind College of Pharmacy, Jaipur, Rajasthan, India is acknowledged for providing research facilities. We are also grateful to Dr. Reddy Institute of Life Science, Hyderabad, Andhra Pradesh, India for providing spectral data of synthesized compounds. The author VS is thankful to DST, Jaipur for partial financial support (1156/2015).

Compliance with ethical standards

Conflict of interest The authors declare that they have no conflict of interest.

References

Abdel-Aziz M, Metwally KA, Gamal-Eldeen AM, Aly OM (2016) 1,3,4-oxadiazole-2-thione derivatives; novel approach for anticancer and tubulin polymerization inhibitory activities. Anti-Cancer Agents Med Chem 16(9):269–277

Ahsan MJ, Sharma J, Monika S, Jadav SS, Yasmin S (2014) Synthesis and anticancer activity of N-aryl-5-substituted-1,3,4-oxadiazol-2-amine analogues. BioMed Res Inter 2014, Article ID: 814984. http://dx.doi.org/10.1155/2014/814984.

Aydemir N, Bilaloglu R (2003) Genotoxicity of two anticancer drugs, gemcitabine and topotecan, in mouse bone marrow in vivo. Mut Res 537:43–51

Azam F, El-gnidi BA, Alkskas IA (2010) Combating oxidative stress in epilepsy: design, synthesis, quantum chemical studies and anticonvulsant evaluation of 1-(substituted benzylidene/ethylidene)-4-(naphthalen-1-yl)semicarbazides. Eur J Med Chem 45:2817–2826

Bakht MA, Yar MS, Abdel-Hamid SG, Al-Qasoumi SI, Samad A (2010) Molecular properties prediction, synthesis and antimicrobial activity of some newer oxadiazole analogues. Eur J Med Chem 45:5862–5869

Boyd MR, Paull KD (1995) Some practical considerations and applications of the National Cancer Institute in vitro anticancer drug discovery screen. Drug Dev Res 34:91–109

Corona P, Carta A, Loriga M, Vitale G, Paglietti G (2009) Synthesis and in vitro antitumor activity of new quinoxaline derivatives. Eur J Med Chem 44:1579–1591

NCI/NIH (2014) Development therapeutic program NCI/NIH. http://dtp.nci.nih.gov. Accessed 13 November 2014

Finger GC, Dickerson DR, Starr LD, Orlopp DE (1965) Aromatic fluorine compounds. XIII. Substituted N-phenylglycine ethyl esters and hydrazides. J Med Chem 8:405–407. https://ncats.nih.gov/files/ZD4054.pdf. Accessed 18 September 2015

Karabanovich G, Zemanová J, Smutný T, Székely R, Šarkan M, Centárová I, Vocat A, Pávková I, Čonka P, Němeček J, Stolaříkov J, Vejsová M, Vávrová K, Klimešová V, Hrabálek A, Pávek P, Cole ST, Mikušová K, Roh J (2016) Development of 3,5-Dinitrobenzylsulfanyl-1,3,4-oxadiazoles and thiadiazoles as selective antitubercular agents active against replicating and nonreplicating *Mycobacterium tuberculosis*. J Med Chem 59:2362–2380

Khan MU, Akhtar T, Al-Masoudi NA, Stoeckli-Evans H, Hameed S (2012) Synthesis, crystal structure and anti-HIV activity of 2-adamantyl/adamantylmethyl-5-aryl-1,3,4-oxadiazoles. Med Chem 8:1190–1197

Monks A, Scudiero D, Skehan P, Shoemaker R, Paull K, Vistica D, Hose C, Langley J, Cronise P, Vaigro-Wolff A, Gray-Goodrich M, Campbell H, Mayo J, Boyd M (1991) Feasibility of a high-flux anticancer drug screening using a diverse panel of cultured human tumor cell lines. J Natl Cancer Inst 83:757–766

Prabhakaran V, Balasubramanium R, Sathe P, Krishna CM, Juvekar A (2014) In vitro anticancer activity of monosubstituted chalcone derivatives. Int J Tumor The 3:1–9

Rajak H, Thakur BS, Singh A, Raghuvanshi K, Sah AK, Veerasamy R, Sharma PC, Pawar RS, Kharya MD (2013) Novel limonene and citral based 2,5-disubstituted-1,3,4-oxadiazoles: a natural product coupled approach to semicarbazones for antiepileptic activity. Bioorg Med Chem Lett 23:864–868

Ramaprasad GC, Kalluraya B, Kumar BS, Mallaya S (2013) Synthesis of new oxadiazole derivatives as anti-inflammatory, analgesic, and antimicrobial agents. Med Chem Res 22:5381–5389

Sangshetti JN, Chabukswar AR, Shinde DB (2011) Microwave assisted one pot synthesis of some novel 2,5-disubstituted 1,3,4-oxadiazoles as antifungal agents. Bioorg Med Chem Lett 21:444–448

Shoemaker RH (2006) The NCI60 human tumour cell line anticancer drug screen. Nat Rev Cancer 6:813–823

Siegel RL, Miller DK, Jemal A (2015) Cancer statistics, 2015. CA Cancer J Clin 65:5–29

Takiar R, Nadiyal D, Nandakumar A (2010) Projections of number of cancer cases in India (2010-2020) by cancer groups. Asian Pac J Can Pre 11:1045–1049

Tuma MC, Malikzay A, Ouyang X, Surguladze D, Fleming J, Mitelman S, Camara M, Finnerty B, Doody J, Chekler EL, Kussie P, Tonra JR (2010) Antitumor activity of IMC-038525, a novel oral tubulin polymerization inhibitor. Transl Oncol 3:318–325

Vichai V, Kirtikara K (2006) Sulforhodamine B colorimetric assay for cytotoxicity screening. Nat Protoc 1:1112–1116

WHO (2014) WHO World Cancer Report. http://www.nydailynews.com/life-style/health/14-million-people-cancer-2012-article-1.1545738. Accessed 12 December 2014

Zhang K, Wang P, Xuan L, Fu X, Jing F, Li S, Liu Y, Chen B (2014) Synthesis and antitumor activities of novel hybrid molecules containing 1,3,4-oxadiazole and 1,3,4-thiadiazole bearing Schiff base moiety. Bioorg Med Chem Lett 24:5154–5156